Cheetah-cub-S: Steering of a Quadruped Robot using Trunk Motion

K. Weinmeister[1], P. Eckert[2], H. Witte[1] and A.-J. Ijspeert[2]

***Abstract*— A reliable concept for steering was realized by integrating a spine-like structure with one DoF into a quadruped robot - Cheetah-cub-S. We increased maneuverability dramatically compared to a robot with rigid spine, while keeping controlling effort low. The robot weights 1160 g at 0.1 m (height), 0.105 m (width) and 0.205 m (length). Based on qualitative tests, it is able to run 0.36 m/s and turn within a radius of 0.51 m (equivalent to 2.48 body lengths) at 0.31 m/s (equivalent to 34°/s). We could steer the quadruped around three objects in a 7.13 m (23 s @ 0.31 m/s) slalom within our test area. Due to its modularity, Cheetah-cub-S is a versatile mobile platform and components such as the spine segment, legs, motors or steering mechanism can be exchanged, leading to easier development of even higher performing robot-versions.**

***Index Terms*— Quadruped robot, Spine, Turning**

I. Introduction

Search and rescue organizations all over the world employ canine-units to find live or dead humans in areas of disasters. The canine-units are an extremely valuable and unreplacable part of the international search and rescue community. It takes multiple years to train a dog in finding people by smell and hearing and not to be afraid in unforeseen situations. The fact that dogs are living beings and friends to their trainers as well as this high investment to train them make them very valuable. Thus they will not be sent into situations where potential danger for their life is present. Here robots can fill the gap and do preliminary recon to define if more detailed search by the human and animal rescuers makes sense. This boosts efficiency of the search and might save lifes. For robots to be able to join such missions versatility is a must. This project focuses on increasing the abilities of Cheetah-Cub [12], a compliant quadruped robot and to bring it one step further towards application. Cheetah-cub focuses on its leg design, an advanced spring loaded pantograph leg (ASLP-leg) [13], following the model of small quadrupedal mammals [15]. Due to its passive compliant properties, effects like self-stabilization during open loop locomotion could be observed. However, one feature that was missing and is crucial for future application to search and rescue is the ability to steer. The only possibility to steer without adding additional degrees of freedom (DOF) is by strong modulation of the locomotion regime. Inspired by properties of mammalian-like locomotion advantageous for robot motion [16], we want to make use of an actuated spine to improve Cheetah-cubs steering ability and thus bring it one step closer to future field application. The implemented mechanism should hereby be as simple as possible and show a good tradeoff between dynamic speeds, robust mechanics and low cost in control. Aiming at a small scale system, actual cost can be kept to a minimum (under 1500 US-Dollar and even drop lower with higher production numbers), which makes wide distribution of the robots possible. Additionally, systems could be left in the researched, dangerous areas without straining the financial aspect of the search too much.

In the past, different robots with a spine-like structure were introduced. In 1996, a planar quadruped robot of the MIT used an articulated spine during bounding to improve its locomotion [6]. It was shown that flexing the spine augmented the thrust provided by the legs. In contrast, a fully passive and compliant mobile platform was developed by Kani and co-workers in 2011. Three different spine types were tested and Fanari was able to gallop down a slope just using gravity [4]. Different spine designs were also investigated by Eckert in the modular, compliant quadruped Lynx [3]. Again, the role of the spine during bounding was investigated by camera recordings. A parallel actuated compliant spine was implemented into the "open loop quadruped" Canid to analyse the role of the spine during bounding and galloping [10]. Due to open loop, touchdowns were uncoordinated and no useable bounding gait could be achieved.

To sum up, all these spines were designed to improve forward locomotion while only vertical bending was allowed. Therefore, turning has to be done based on other ideas, e.g. by modulating individual foot placement which is done by robots with a rigid body i.e. no spine and legs with a high degree of freedom (DoF). Matos and Santos applied a CPG algorithm to a SONY Aibo to make omnidirectional locomotion possible by controlling each leg individually [7]. BigDog is another quadruped which uses ab-/adduction of the legs to change direction [11]. Ajallooeian and co-workers developed a controller for a cat-sized quadruped robot and made turning motion possible by using ab-/adduction at the hip [1]. Tekken4 has four legs with a DoF of four each and is able to change direction by adapting the yaw angle of each leg [5]. All in all, changing directions with a rigid spine is possible but requires an overall high DoF (especially hip ab-/adduction) of the legs and thus multiple controlling structures. These robots also need the ab-/adduction for a different reason. They are all relatively heavy and if no or little ground clearance is achieved during turning, high stress on the joints can occur and break them. As Cheetah-cub is very lightweight it is possible to go for different solutions. Never the less, such stress could occur and thus it should be kept in mind during the design process.

Finally, Zhao and co-workers developed a multi-segment,

[1]Chair of Biomechatronics, Faculty of Mechanical Engineering, Technische Universit"at Ilmenau, Germany

[2]Biorobotics Laboratory, Ecole Polytechnique Federale de Lausanne, Switzerland

biologically inspired and compliant spine and embedded it into a quadruped robot. Due to a sine wave motion of the spine and an asymmetrical friction material at the feet, the robot was able to move forward. Turning was also possible by applying lateral bending to the spine. Therefore, the robot achieved an average angular speed up to 6.2 °/s [14]. This approach seems to be very promising but requires complex parts, actuation and does not move dynamically.

Furthermore, we should have a look at robots based on amphibians and reptiles because for them lateral bending is crucial. Pleurobot [8] and Salamandra robotica II [2] are two bio-inspired salamander-like robots. Both are able to walk on the ground and to swim. The former has 27 and the latter 12 actuated DoFs. Instead of increasing the overall complexity by increased DoF and controlling algorithms to place the feet individually, we aimed for keeping the control structure as simple as possible while implementing intelligent mechanics.

II. Concept

The spine is located symmetrically between two trunk-modules and is composed of an active (motor) and compliant joint (Fig. 1). Deflection can be determined actively while external loads are partially absorbed by the compliant element.

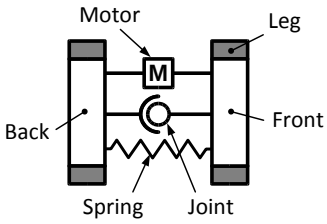

Fig. 1. Basic concept: Active and compliant joint with motor, joint and spring in parallel placed central between fore and hind trunk-module

Fig. 2A shows a top view at neutral position. To achieve the active bending, a motor (M) was placed in the center of the structure to bend both fore and hind trunk-modules synchronously and equally towards one side via a cable mechanism (Dashed lines). One leaf spring (Green line) was attached to each side of the motor. The overall turning radius is reduced compared to having only one spring on a particular side. Fig. 2B shows the bending of both leaf springs due to the activated motor.

III. Cheetah-cub-S

Based on the previously detailed concept, a prototype was developed to test the approach, and to identify possible sources of deficiencies. After clearing, the final version of Cheetah-cub-S was developed and tested for turning.

A. Materials

The robot consists of different materials due to variable material properties that influence the usefulness for the structural parts.

Polyoxymethylen (POM): was milled for the leaf springs to enable large amount of elastic deflection at low weight.

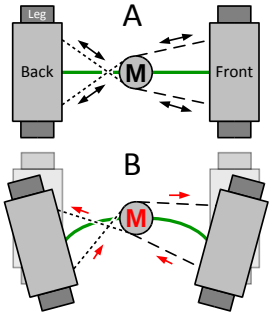

Fig. 2. A: General setup at neutral position (top-view), B: Motor turns clockwise to initialize curved path; M - Motor (black = neutral, red = powered), Dashed line - Cable mechanism, Arrows - Movement of cables, Green line - leaf spring;

Carbon fiber reinforced plastic (CFRP) and *Glass fiber reinforced plastics (GFRP):* were used to create the leg-units and trunk modules, that have to withstand high stress and should not be flexible. *3D printed plastics (ABS):* found their usage where the complex parts would have been difficult or expensive to produce with classical methods and no big stress was foreseen.

B. Spine segment

The center of the spine is the servo-motor for active bending of the coupled leaf springs who in turn connect the spine-motor with both trunk modules. The springs are dimensioned to avoid bending due to gravity and thus, to allow lateral bending only. Furthermore, to decrease externally induced torsion, two leaf springs were mounted in parallel (Fig. 3). The torque of the motor is transferred by a cable-mechanism to enable the deflection which initializes the turning motion.

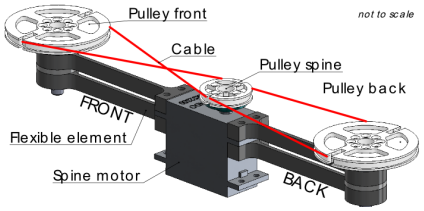

Fig. 3. Spine design: Isometric and section view - clarified CAD model (without screws, etc.)

C. Leg unit

Each trunk part consist of two leg units. The legs were taken from the role model Cheetah-cub and paired via a CFRP plate to create fore and hind trunk modules. These modules were the same but turned 180° against one another. Fig. 4 shows the ASLP-leg design and one leg unit. The pantograph leg mechanism consists of four segments and is driven by two motors: One for the hip (directly) and the other one for the knee joint (via cable).

Fig. 5 shows the prototype with all electrical cabeling connected to the control board (RoBoard RB110, OS: Linux Xenomai) whereas the power supply continues externally. On the top of the spine structure, a handle is mounted to simplify the usability during experiments.

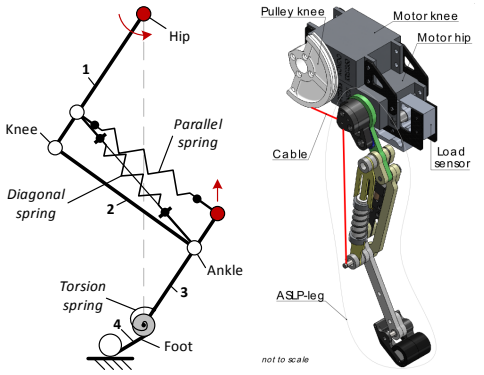

Fig. 4. Left: Four segment advanced spring loaded pantograph: 1 → Scapula, 2 → Humerus, 3 → Radius, 4 → Foot, Red - Actuation [12], following [15]; Right: Leg unit - clarified CAD model (without screws, etc.): ASLP-leg - Advanced spring loaded pantograph leg

D. Range of motion

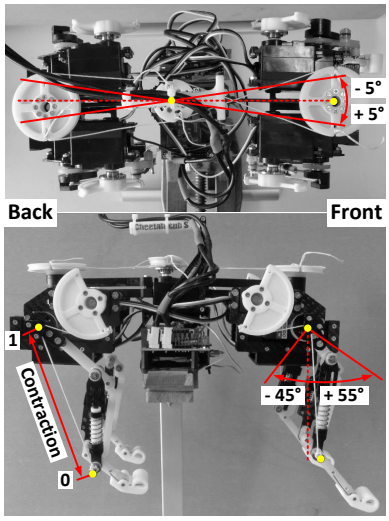

Fig. 5. Range of motion: Top - Spine: ±10°; Bottom right - Hip: +55°/-45° (Front legs)and ±45° (Hind legs); Bottom left - Knee: Full (1) or no (0) contraction of the diagonal spring; Reference points: hip/spine motor and ankle/trunk joint (yellow)

To ensure a synchronous movement of hip and knee with respect to spine actuation, a calibration of the postition controlled servo-motors was done. Fig. 5 shows the respective ranges of motion. Each spine segment bends to ±5° which corresponds to a total spine deflection of ±10°. The positive spine angle represents turning to the right and negative to the left.

E. Gait

The original trotting gait parameters of Cheetah-cub are used and implemented in an open loop CPG-network. The front left and hind right leg move synchronously as well as the front right and hind left leg (trot= diagonal gait). Furthermore, while one pair of feet touches the ground the other does not.

F. Deficiencies in the prototype

Torsion: The spine segments were not able to prevent external torsion sufficiently which resulted in unsuccessful locomotion. Fig. 6 shows examples of manually produced spine twists.

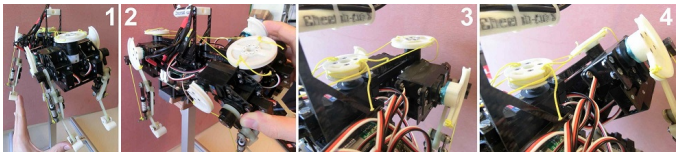

Fig. 6. Examples of high spine torsion: 1 - Front and back pushed by hand, 2 - Front only, 3 and 4 - Comparison back part

The first picture shows the situation with both parts rotated against each other. To minimize torsion, the overall height and stiffness of the leaf springs was increased by implementing a third one in parallel. The segment was added at the bottom of the robot to prevent extensive redesign. The amount of torsion was reduced significantly which improved the overall performance.

Ground contact: During the first experiments, more sliding than expected was observed. Duct tape for front and sand paper for hind legs were added to improve the performance. This was mostly successful.

Sag of cables and steering mechanism: The original idea of steering via cables was suboptimal due to missing structures for keeping tension at all time. The cables sagged which led to undesired backlash. Instead of implementing additional components, the cables were replaced by four rigid bars and the pulleys by simple levers. Figure 7 shows the corresponding setup.

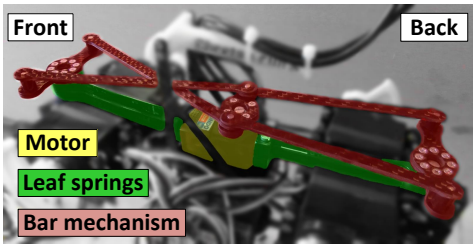

Fig. 7. Final spine-like structure: Setup of the motor (yellow), leaf springs (green) and bar mechanism (red)

Due to the small range of the spine angle , the rigid bars never go into a singularity. As a side effect we could observe additional stiffening against torsion while keeping loss of backdrivability to a minimum.

IV. EXPERIMENTS

Based on the previous design process and final redesign, the Cheetah-cub-S (Fig. 7) was developed and used to steer via trunk motion.

A. Setup

To evaluate the performance on turning, the trajectory of the movement was observed within the test area of

4.5 m x 2.8 m by 14 infrared light cameras of the motion capture system (MOCAP) from OptiTrack at 240 frames per second (fps). The robot was connected via SSH to start the onboard running CPG and to steer the robot by setting an offset to the spine-motor. A cable was used to power Cheetah-cub-S.

B. Procedure and radius calculation

The spine deflection was divided into steps of two degrees, i.e. from -10°to 10°. At each deflection, ten attempts with a minimum of two complete circles were recorded. If the turning radius exceeded the test area, the robot had walked as far as the movement was recordable. Furthermore, attempts were marked as not successful if the robot fell over. To evaluate the experiments, we calculated the theoretical turning radius and used it as a comparison to the real performed one. The calculation of the turning radius is based on the simplified robot ("Single Track Model" used in automotive construction) and its geometrical constraints. Fig. 8 shows the sketch which was used to derive the following equations.

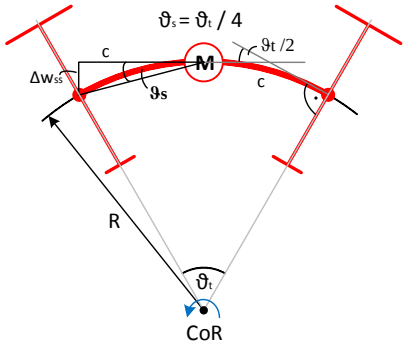

Fig. 8. Calculation of radius based on spine angle: M - Motor, CoR - Centre of rotation, R - Turning radius, c - Half shoulder to shoulder distance, Δwss - Deflection regarding bending force of motor, ϑ_t - Turning angle, ϑ_s - Spine angle

The robot is shown with a bent spine while turning counter clockwise. The motor (M) separates front and back (c) while the turning radius (R) indicates the bent spine with a deflection (Δw_{ss}). Due to geometrical constraints, the turning angle (ϑ_t) is four times the spine angle (ϑ_s). Finally, the turning radius (R) is expressed in radian and calculated by (3).

$$\vartheta_t{}^{rad} = \frac{2*c}{R}; \quad R = \frac{2*c}{\vartheta_t{}^{rad}} \tag{1}$$

$$\vartheta_t{}^{rad} = \frac{2*\pi*\vartheta_t{}^{deg}}{360°}; \quad \vartheta_t{}^{deg} = \vartheta_s{}^{deg}*4 \tag{2}$$

$$R = \frac{2*c*360°}{2*\pi*\vartheta_t{}^{deg}}; \quad R = \frac{c*90°}{\pi*\vartheta_s{}^{deg}} \tag{3}$$

C. Turning and its analysis

One of the top markers was used to analyze the turning motion regarding radius and velocity. The experimental radius was calculated by two algorithms with the help of MATLAB (R2014a). First, if at least one full circle was achieved, the center of rotation (CoR) was calculated by the average values for direction x and y. Based on this point, the radius to each point of the trajectory was calculated by the euclidean distance. The average and the standard deviation of all distances was used for the mean radius and its deviation. This was done at high spine deflection: 10°, 8°, 6°, 4°& -10°. Second, if no full turning motion was recorded, the calculation was done by a predefined MATLAB-function (CircleFitByPratt.m [9]) based on Newton's approximation method. The circle was fitted to the trajectory. The average and standard deviation of all radii was used for the mean radius and its variation. This algorithm was used for all other spine deflection: 2°, 0°, -2°, -4°, -6°& -8°. The mean velocity was calculated by the total distance traveled divided by the observed time frame which was kept constant for all runs at each deflection to simplify the evaluation.

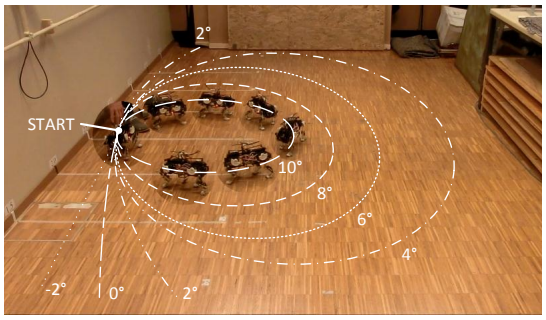

Fig. 9. Simplified trajectory of different spine deflections: Full turning up to 4°, negative spine deflections were left out due to clarity

Cheetah-cub-S trots different circle radii with decreased angles. The test area is not sufficiently big for all the deflections, thus results were approximated with the above mentioned method during the analysis. With focus on the sharpest turning motion, the robot achieves its minimum radius at one run at 10° spine deflection of 0.51 +/- 0.07 m at 0.31 m/s. Fig. 10 illustrates an exemplary single attempt of Cheetah-cub-S with 10° spine deflection. The four turns occur clockwise from start to end position in about 39 s.

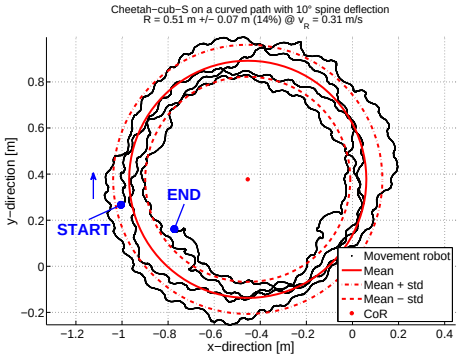

Fig. 10. One exemplary single attempt of Cheetah-cub-S with 10° spine deflection, ∼4 clockwise turns from start (-1, 0.25) to end (-0.75, 0.15) point

The bidirectional swinging occurred due to the inherent perturbations during the trotting gait. The calculated CoR,

mean radius and corresponding standard deviation are shown in red. Furthermore, basic parameters (Spine deflection, radius and velocity) were given to simplify the classification.

97% of all 110 runs were successful because Cheetah-cub-S fell over only when it hit the wall. This happened mostly at very small spine deflections because the starting point was close to the wall and due to variations at the touch down, the robot sometimes tended to walk towards the border. The overall results are illustrated in Fig. 11.

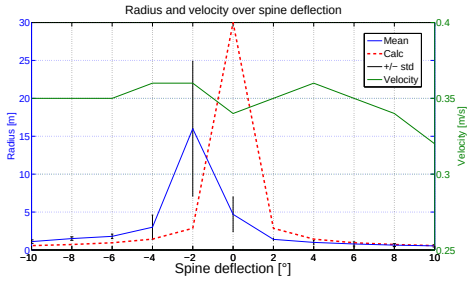

Fig. 11. Results of experiments: Radius and velocity over spine deflection: Calc - calculated radii (30 m at 0° represents ∞), std - standard deviation

The radius peaks at -2°, decreases and levels out towards greater spine deflection because the larger the angle the smaller the radius (see 3, p. 4). An asymmetry exists by comparing mean and calculated radii. It is due to minor backlash of the steering mechanism caused by some plastic deformation of the leaf spring after testing. Thus the spine tends to have a small offset to one side than the other. As a consequence the experimental radii are smaller than the calculated ones for positive deflections.

The maximum velocity of 0.36 m/s was reached at straight locomotion and decreased slightly with greater spine deflection. The ground had the most determining effect on propulsion because of its structure. Parquet made out of small wood pieces created a slight anisotropic friction and thus influences the overall speed. In addition, tape was used as markers in other experiments done in parallel which changed the friction locally. The low friction between feet and ground and the non-optimized gait caused sliding motion which increased with greater spine deflection due to additional dynamic forces, e.g. centrifugal force. Never the less, optimizing the gait would have somewhat clouded the comparison to the old robot Cheetah-cub and thus this is kept as part of future investigations into the topic. Cheetah-cub's ability to turn, induced by markedly changing the gait parameters, i.e. amplitude of hip actuation, was tested. The necessary differences in amplitude of inner and outer leg were calculated based on distance of each leg towards the CoR. The same phenomenon can be seen by considering a car and its wheels when it drives on a curved path. The outer wheel spins faster than the inner one. The calculated amplitude of the inner leg had to be 20 % less than the outer to achieve a radius of 0.5m. No changes in direction occurred. The reason was the high frequency which made it impossible for the servo-motors to reach the desired amplitudes. Small changes had no effect on the real locomotion. The frequency was not lowered to keep the comparison between the two robots. To achieve similar radius the amplitudes were set to zero and then increased until the desired motion occurred. The following figure 12 shows the result of Cheetah-cub turning (R≈0.5 m) with an amplitude ratio of 5°(inside) to 50°(outside).

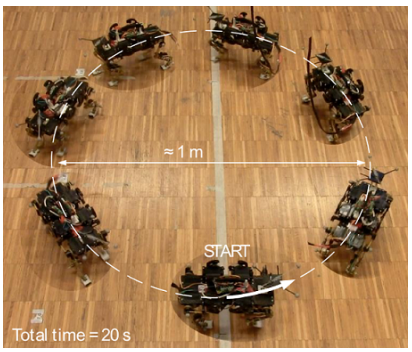

Fig. 12. Cheetah-cub turning clockwise with an amplitude ratio of 5° to 50°: R≈0.5 m

The full circle was completed after 20 s which correlates to ≈0.16 m/s. The velocity was half the one of Cheetah-cub-S and the gait changed dramatically. The predefined trot changed to a full contact sliding gait because of the small amplitudes and made it sensitive to the surface quality. The differences in amplitude of calculation and reality were disproportional. One cause could be the nature of the implemented foot trajectory. The calculated amplitudes correlated to the distance during stance-phase (wheel-model with full time contact) but in reality the foot touched the ground less. To achieve the desired ground contact, the foot trajectory has to be controlled and adjusted during locomotion.

V. Slalom-run

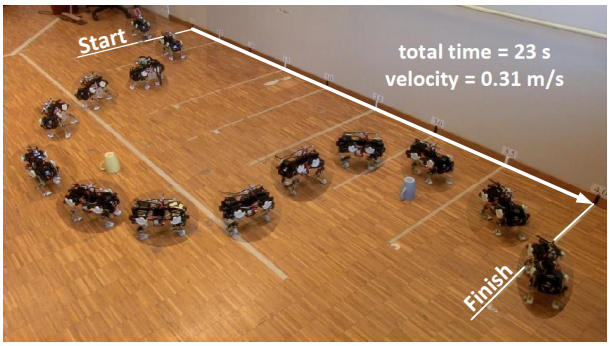

Fig. 13. Slalom - Experiment: Recorded movement of Cheetah-cub-S represented by snapshots (without cable), white arrow represents 4 m distance

An additional task was to move around three objects by two clockwise and one counter clockwise turn. This was a little closer to a real life scenario, as full turns happen rather rarely. The start and finish line were four meters apart and within the objects were spread symmetrically. Fig. 13 shows the recorded movement in snapshots. The robot can

be steered by a user to solve a certain task. Cheetah-cub-S succeeded nicely, which gives additional weight to the usefulness of a bendable spine.

VI. CONCLUSION

With the help of the artificial spine, the turning radius was reduced to 0.51 m ($\approx$ 2.48 BLs) at 0.31 m/s. The design allowed a human operator (or a higher-level navigation controller) to modulate the spine deflection and therefore to steer the robot in its environment.

TABLE I
COMPARISON OF CHEETAH-CUB AND CHEETAH-CUB-S

Properties	Cheetah-cub-S	Cheetah-cub
Mass [g]	1160	1100
Height [m]	0.1	0.1
Width [m]	0.105	0.1
Length [m]	0.205	0.205
Max. forward velocity [m/s]	0.36	1.42
Max. turning velocity [°/s]	34[4]	18

In comparison to Cheetah-Cub, the dimensions are similar apart from the mass, forward and turning velocity. Although the additional weight of 60 g, caused by the spine actuator, Cheetah-Cub-S is able to almost turn twice as fast as Cheetah-Cub and keep most of the characteristics of a normal trotting gait. For us, it is a excellent trade-off between increase in maneuverability and keeping the mechanical and computational complexity low. The forward speed decreased drastically, caused by the non-optimized gait and much lower supply voltage than Cheetah-Cub (9V instead of 14V). This has to be improved in a future version to make effective search possible. Cheetah-cub-S introduces a reliable approach to enable steering via trunk motion without the consideration of individual foot placement or gait specialization. We implemented only one additional DoF but increased the maneuverability markedly even though the locomotion is not optimized yet. If we go back now and take a look at our natural role-models, cats and dogs, we find that a combination of ab-/adduction is strongly used for turning. The legs hereby induce the turning motion and the flexible spine is used to lower the turning radii and provide more muscle-force for dynamic maneuvers. We should and will in the future combine these to successful mechanisms into one to study how it can improve the versatility even further. Cheetah-cub-S is one step closer to field application, but many more have to be taken to reach this goal. Sensors to detect the environment and survivors as well a robust mechanisms to fall and recover, move down and up stairs, slopes as well as robustness against dust and water as well as reliable communication methods have to be added. With our Cheetah-cub platforms, we hope to build robots that are easy to use, effective and cheap enough to perform wide range searches with multiple robots on the ground as well as having the realistic choice to abandon the robot if recovery would be too dangerous.

[4]Min. radius of 0.54 m @ 0.31 m/s

ACKNOWLEDGMENT

We thank all members of Biomechatronics and BioRob groups for their advice and support.

REFERENCES

[1] Ajallooeian, M.; Pouya, S.; Sproewitz, A. and Ijspeert, A. J.: Central pattern generators augmented with virtual model control for quadruped rough terrain locomotion. In IEEE International Conference on Robotics and Automation (ICRA), pp. 3321 - 3328, 2013

[2] Crespi, A., Karakasiliotis, K., Guignard, A. and Ijspeert, A. J.: Salamandra robotica II : an amphibious robot to study salamander-like swimming and walking gaits. In IEEE Transactions on Robotics, Vol. 29, Num. 2, p. 308 - 320, 2013

[3] P. Eckert, A. Sprwitz, H. Witte and A. Ijspeert. Comparing the effect of different spine and leg designs for a small bounding quadruped robot. ICRA 2015, Seattle, Washington, USA, 2015.

[4] Kani, M. H. H.; Derafshian, M.; Bidgoly, H. J. and Ahmadabadi, M. N.: Effect of flexible spine on stability of a passive quadruped robot. In IEEE International Conference on Robotics and Biomimetics (ROBIO), pp. 2793 - 2798, 2011

[5] Kimura, H.; Fukuoka, Y. and Katabuti, H.: Mechanical Design of a Quadruped "Tekken3&4" and Navigation System Using Laser Range Sensor. In INTERNATIONAL SYMPOSIUM ON ROBOTICS, Vol. 36, pp. 10, 2005

[6] Leeser, K.F.: Locomotion Experiments on a Planar Quadruped Robot with Articulated Spine. Master's thesis, 1996

[7] Matos, V. and Santos, C. P.: Omnidirectional locomotion in a quadruped robot: a cpg-based approach. In IEEE/RSJ International Conference on Intelligent Robots and Systems (IROS), pp. 3392 - 3397, 2010

[8] Pleurobot. url: http://biorob.epfl.ch/pleurobot. Visited on 29.09.2014

[9] Pratt, V.: Direct least-squares fitting of algebraic surfaces. In Computer Graphics, Vol. 21, pp. 145 - 152, 1987

[10] Pusey, J. L.; Duperret, J. M.; Haynes, G. C.; Knopf, R. and Koditschek, D. E.: Free-Standing Leaping Experiments with a Power-Autonomous, Elastic-Spined Quadruped. In SPIE Defense, Security, and Sensing, 2013

[11] Raibert, M.; Blankespoor, K.; Nelson, G. and Playter, R.: The Big-Dog Team (2008): Bigdog, the rough-terrain quadruped robot. Proceedings of the 17th World Congress - The International Federation of Automatic Control, 2008

[12] Sprowitz, A.; Tuleu, A.; Vespignani, M.; Ajallooeian, M.; Badri, E. and Ijspeert, A.: Towards Dynamic Trot Gait Locomotion: Design, Control, and Experiments with Cheetah-cub, a Compliant Quadruped Robot. In International Journal of Robotics Research, Volume 32, Issue 8, July 2013, pp. 933 - 951

[13] Witte, H.; Hackert, R.; Ilg, W.; Biltzinger, J.; Schilling, N.; Biedermann, F.; Jergas, M.; Preuschoft, H. and Fischer, M.: Quadrupedal mammals as paragons for walking machines. International Symposium on Adaptive Motion of Animals and Machines (AMAM2000), Montreal, Canada, 2000

[14] Zhao, Q.; Sumioka, H. and Pfeifer, R.: The effect of morphology on the spinal engine driven locomotion in a quadruped robot. In The 5th International Symposium on Adaptive Motion of Animals and Machines (AMAM2011), pp. 51 - 52, 2011

[15] Fischer, M. S. and Witte, H.: The functional morphology of the three-segmented limb of mammals and its specialities in small and medium-sized mammals. In Proc. Europ. Mechanics Coll. Euromech 375 Biology and Technology of Walking, pp. 10-17,1998

[16] Witte, H., Ilg, W., Eckert, M., Hackert, R., Schilling, N., Wittenburg, J., Dillmann, R. and Fischer, M. S.: Konstruktion vierbeiniger Laufmaschinen. VDI-Konstruktion 9-2000, pp. 46 50, 2000

[17] Mmpel, J., Eisold, R., Kempf, W., Schilling, C. and Witte, H.: A Modular Concept for a Biologically Inspired Robot. In Robot Motion and Control 2009, pp. 391-400, Springer London, 2009